Fermilab

TM-1048
8055.000
June 1981

THE PROTON BEAM SWEEPING SYSTEM FOR AN ANTIPROTON TARGET STATION USING LITHIUM LENSES

T. Vsevolzhskaya, G. Silvestrov, A. Chernyakin
Institute for Nuclear Physics, Novosibirsk

J. MacLachlan
Fermi National Accelerator Laboratory, Batavia, Illinois

The mass depletion of the target through fast heating and shock formation by the action of an intense proton beam focused to a very small spot is the principal obstacle to obtaining optimum antiproton production. It is shown in reference (1) that for a fixed antiproton acceptance $\varepsilon<<\varepsilon_0=\lambda<\theta_0^2>/2\sqrt{3}$ there are quite definite optima for target length ℓ_{opt}, proton beam size $(\sqrt{<r_p^2>})_{opt}=\sqrt{2}\,\sigma_{opt}$, and antiproton collection angle $\theta_{C\,opt}$. The quantity ε_0 is an antiproton emittance characteristic of a target of length ℓ_T equal to the nuclear absorption length λ, when the mean square production angle is $<\theta_0^2>$. The dependence of the capture efficiency on proton beam size, target length, and $\bar{p}$ collection angle are shown in Figures 1, 2, and 3 respectively for the parameters $p_{\bar{p}}=5.4$ GeV/c, $\varepsilon=5\pi\times10^{-6}$m, $\sqrt{<\theta_0^2>}\sim0.1$, $\varepsilon_0\sim3\times10^{-4}$ πm applicable to the Fermilab Tevatron I project. The optimum condition corresponds to the parameters $\sqrt{<r_p^2>}\approx0.05$ mm, $\ell_T\approx2.5$ cm, and $\theta_C\approx0.04$. For 1.8 μs beam spill of 2×10^{13} protons, target heating on the beam axis is greater than 1 ev (12000°K) and 90% depletion of the mass occurs already by ~0.5 μs (2,3). One way to avoid this phenomenon is to move the proton beam across the target at a velocity greater than the shock wave velocity and synchronously move the antiproton acceptance. This idea of sweeping the proton beam was proposed in a Fermilab $\bar{p}$ note of Krienen and Mills (4).

In the following we consider several practical approaches to implementing the sweeping scheme for a target station with a lithium lens for proton beam focusing and a lithium lens as antiproton collector. By this scheme it becomes possible to employ the focusing which gives optimum $\bar{p}$ production efficiency with the high intensity necessary for the desired net yield. This scheme serves not only to avoid the target mass depletion problem but reduces the proton beam destruction of the beryllium entrance window of the collection lens. Before the sweeping idea was introduced it was proposed to protect the collection lens entrance window by using an extremely short focus proton beam lens so that the protons would diverge from the target at the widest possible angle and to move the collection lens as far downstream as necessary to preserve it. Both of these measures complicate the design and the second, particularly, decreases the collection efficiency.

The proton beam lithium lens has length ℓ_1=10 cm, B_{max}=130 kG, and aperture radius a_1=2.5 mm. The focal length is F_1=50 cm at 80 GeV. For proton beam emittance $\varepsilon=5\times10^{-8}$ πm (5) and a required beam spot size r_p=0.05 mm, the beam envelope function β is $\beta=r_p^2/2\varepsilon$=2.5 cm and convergence angle $\alpha_c=\sqrt{\varepsilon/\pi\beta}=1.4\times10^{-3}$. Thus β at the beam window of the lens will be $\beta_\ell=\beta_0+F_1^2/\beta_0$=10 m, and the beam size will be r_p=1 mm so that there is considerable extra aperture. This reserve could prove useful if beam manipulation in the main ring or during extraction should result in increased emittance. The collection lens has length ℓ_2=7 cm, B_{max}=140 kG, aperture radius a_2=5 mm. For a collection momentum $p_{\bar{p}}$=5.4 GeV/c, the focal length is F_2=10 cm and the acceptance angle $\theta_c=\pm50$ mrad is near to optimum. Together these lenses achieve practically optimum focusing and collection; the system loss of ~15% from ideal is due mainly to nuclear absorption in the lenses. It was shown in ref. (2) that with conventional quadrupole focusing the limit on the proton spot size is $\sigma_p\approx0.2$ mm because of aberrations.

Choice of Sweep Velocity

If the dependence of target density on time is known for the chosen proton beam parameters we can estimate the sweep velocity necessary to achieve a specified fraction of the production expected for constant target density. Curves taken from reference (6) for the change of density on the proton beam axis are shown in Figs. 4a and 4b. These curves were obtained by solving the equations of state in the region of beam heating at the initial stage of material motion behind the shock front using the Hugoneu shock adiabats for a plane shock which determine the velocity u from its dependence on the pressure, P=H(u) (7). This approach describes quite well the early stage of such a process in the domain $\gamma/\gamma_0>0.5$ where the density γ is not too different from the initial value. In this region, which is our principal region of interest, the results for Pb agree well with the curves given in ref. (3) shown as the solid curve in Fig. 4a. In this calculation the 1.8 μs beam pulse contained 2×10^{13} protons. The energy loss dE/dx=1.6 MeV gm^{-1}cm^2 so that the heating is $q=9\times10^{12}/(r_p \text{ cm})^2$ erg/gm sec. One can see that at σ_p=.05 mm the difference between the curves for Pb and W is not so great; the time to decrease the density by 50% is .08 μs for Pb and .135 μs for W. These similar results arise from the compensating effects of the difference in sound velocity between Pb and W (u_s (Pb)=2000 m/s, u_s (W)=4000 m/s) and the difference in heat of fusion (Q_m (Pb)=4.77 kJ/mole, Q_m (W)=35.2 kJ/mole). It is interesting to note that for tungsten the density has already dropped to 50% by the time that the metal has reached the boiling point and that more than half of the deposited energy has been carried away by the shock wave. The velocity of the material on the shock front is $u_{sh}\approx350$ m/s. The decrease of the mean value of the target density is shown by the dashed line in Fig. 4b. One can see that $\bar{p}$ production is down by about 10% already at Δt=.08 μs; to prevent greater loss one should move the beam with velocity $v_b=2\sigma_p/\Delta t$=1.2 mm/$u_s>>u_{sh}$. Total beam displacement on a W target should be $\Delta_{tgt}\geq2.16$ mm ~ ±1.1 mm.

Sweeping Schemes

Fast beam displacement can be carried out by means of a pulsed magnet with a linearly varying alternating field placed upstream of the proton beam lens providing a deflection of $\alpha_1 = \pm \Delta_{tgt}/F_1 = \pm 2.2 \times 10^{-3}$. Thus, the field integral for the deflecting magnet should be $\int B\, d\ell = 5.87$ kG m. It is easily shown that the displacement at the target does not depend on the distance d_1 from the deflecting magnet to the center of the lens and that for any d_1, $\Delta_{tgt} = \alpha_1 F_1$. The angle of the beam leaving the target is $\alpha_2 = (1 - d_1/F_1)\alpha_1$ so that by placing the deflection magnet center on the first focal plane ($d_1 = F_1$) one obtains a parallel displacement of the beam on the target. However, this condition is not so important; the value of d_1 can be varied from $d_1 = 0$ to $d_1 \sim (2\text{-}4) \times F_1$. The limit on d_1 is that α_2 should be much less than the angular acceptance for $\bar{p}$, $\alpha_2 << \theta \sim 50$ mrad. For larger angle α_2 more collector aperture is required. A stronger limit is placed on d_1 by the displacement Δ_1 across the aperture of the proton beam lens because $\Delta_1 = \alpha_1 d_1$ and because this lens has smaller aperture. It is desirable therefore, to have $d_1 \to 0$ to avoid beam loss. While it is possible to place the magnet downstream of the lens, it does lead to increase in α_1 such that $\alpha_1 > \Delta_{tgt}/F_1$. A case in which $d_1 = 0$ and the beam arrives at the center of the target off axis by an additional angle $\alpha_2 = \alpha_1$ can be arranged by placing two magnets upstream of the proton lens. The first magnet deflects the beam from the axis by an angle α_3. The second magnet compensates this angle by deflecting an angle $\alpha_1 + \alpha_3$ to direct the beam onto the target through the lens center. This scheme can be implemented, for example, by two magnets with B=15 kG and lengths $\ell_1 = 40$ cm, $\ell_2 = 80$ cm placed directly upstream of the lithium lens so that $\alpha_1 = \alpha_2 = \alpha_3$. In this version we conserve lens aperture at the cost of increasing the total deflecting angle by a factor of three.

It may be a more convenient alternative to sweep the beam in a circle of radius $r_{tgt} = \Delta_{tgt}/\pi = 0.35$ mm or, say, .4 mm for a little safety margin. Two magnets excited $\pi/2$ out of phase by sinesoidal current with a period exactly equal to the spill time of 1.8 μs will produce the circular deflection. For the required deflection angle $\alpha_1 = 0.8$ mrad the magnets must have a field integral of 2.1 kG m. Because this variant looks the most convenient and most elegant we consider it in detail. For instance, two 18 kG magnets of length $\ell_1 = \ell_2 = 12$ cm located directly adjacent to the lens could be used. The aperture of these magnets need hardly be any larger than the lens aperture, perhaps 6 mm x 6 mm. The angle of proton beam incidence on the target, $\alpha_2 < .8$ mrad, can be neglected in the following. Though it might appear that the use of a short focal length lens complicates the sweeping system, note that if the focal length of the lens is increased both deflecting magnet and lens apertures must be increased with a result that stored energy in the magnetic field is the same.

The parallel displacement of the proton beam on the target by $\pm\Delta_{tgt}$ results in an angle $\alpha_{\bar{p}} = \pm \Delta_{tgt}/r2$ for the antiproton beam axis at the second focus. There are two ways to compensate. The first approach is to use a pair of magnets. The first magnet a distance d downstream of the collector receives the beam at an angle of $\alpha_{\bar{p}}$ and displacement $\Delta_d = \alpha_{\bar{p}}\,(d - F_2)$. This

magnet provides a deflection $\sim 2\alpha_{\bar{p}}$ to direct the beam to the center of the second magnet which corrects the angle. A single magnet can be employed if it is located at the focus of the lens and provides the deflection $\alpha_{\bar{p}}$ to correct the angle. The first case has much more freedom in the length and placement of the magnets; for the second case the magnet has to be very close to the lens and there are strong constraints on magnet parameters and design.

The longitudinal displacement of the magnet center from the focus by amount Δx allows complete compensation of the angle error of the beam centroid but results in some mismatch between beam and channel acceptance. Results of a numerical simulation calculation of dependence of the capture efficiency on the mistmatch expressed in units of $\Delta x/F_2$ for displacement $\Delta_{tgt}=\pm 1$ mm are shown in Fig. 5a. One can see that even at $\Delta x/F_2=1$ the losses are only 10%. Figure 5b shows the capture efficiency for one-dimensional transverse sweeping of ± 1 mm versus the tracking error $(B_2-B_1)/B_1$ in the fields of the sweeping magnets for a placement of the proton magnet at the first focus of the proton lens and the antiproton magnet at the second focus of the collector. The solid curve is for $\Delta x/F_2=0$ and the dashed curve gives the result for $\Delta x/F_2=0.5$.

The dependence of capture efficiency on the aperture of the proton lens for a proton beam of large emittance $\varepsilon=3\times 10^{-7}\pi$m is shown in Figs. 6a and 6b for $F_1=40$ cm and $F_1=50$ cm respectively. For all cases ideal compensation of the antiproton beam sweeping is assumed.

For a circular sweeping of the proton beam on a .4 mm radius, two magnets with field integral .72 kG m are needed to produce the deflection $\alpha_{\bar{p}}=4$ mrad which compensates the $\bar{p}$ channel for the source displacement. They may be chosen with a field of 10 kG and lengths $\ell_1=\ell_2=7.2$ cm. The first would be centered at x=10 cm ($\Delta x_1/F_2=0$) and the second at x=20 cm ($\Delta x_2/F_2=1$). In Figure 7 we show the layout for both the proton and antiproton deflecting systems for circular sweeping on a 0.4 mm radius and the proton lens and collector. Compared to the efficiency losses shown in Figs. 5-6 for the significantly greater displacement of ± 1 mm, the loss for the 0.4 mm radius circular sweeping system will be negligible.

Magnet Design

The principal physical and electrical parameters of the magnets are given in the Table.

Table: Sweeping Magnets
for a Targeting System for Proton Beams with
Radius $r_p=0.4$ mm

	α rad	$\int B d\ell$ kG m	$\ell_1=\ell_2$ cm	B_{max} kG	h=w cm	I_{max} kG	L nH	f kHz	V kV	W J
p magnets	$8\cdot 10^{4}$	2.13	11.7	18.0	0.6	8.64	150	560	4.4	5.60
$\bar{p}$ magnets										
a)	4.10^{-4}	0.72	7.2	10.0	1.4	11.2	90	560	3.5	5.65
b)	$4\cdot 10^{-3}$	0.72	5.0	14.4	1.4	16.0	63	560	3.5	8.14

The design and parameters of the magnets are constrained by operating conditions and radiation levels in the target area. From this consideration certain design principles follow:

1) Insulation must be radiation tolerant.
2) Voltages should be kept low.
3) Inductance should be high enough to keep voltage loss on radiation resistant transmission line reasonable.
4) The mechanical structure should be simple, cheap,and reliable.
5) It is useful to simplify all equipment which will be in the radiation area even at the expense of considerable complication of the power supply system which will be in a shielded area.

The magnet parameters listed in the Table were chosen according to these guidelines.

Each magnet consists of a single turn coil with a core of thin (30-50μ) laminated iron. The requirement for field uniformity is not very stringent and is set according to the relative value of the beam displacement as

$$\frac{\Delta B}{B} \quad \frac{\sigma}{\Delta_{tgt}} \sim .1$$

It is easy to show that the voltage required to drive the magnet $V=\omega LI$ depends only on the field integral $\int Bd\ell=\alpha p_{\bar{p}}/300$ but not on the maximum field. In fact, because

$$I = \frac{Bh}{0.4\pi} = \frac{\alpha p_{\bar{p}} h}{120\pi\ell}$$

and

$$L = \frac{4\pi\ell w\times 10^{-9}}{h}$$

one has

$$V = 3.3\times 10^{-11}\ \alpha p_{\bar{p}} w\omega$$

where

I current [A]
B field [kG]
α deflection angle [rad]
$p_{\bar{p}}$ momentum in [eV/c]
h gaps height [cm]
ℓ magnet length [cm]
L inductance [H]
w gap width [cm]
ω pulse angular frequency [s^{-1}]
V maximum driving potential [volt]

Thus, for fixed angle α, aperture, w, and $\bar{p}$ momentum $P_{\bar{p}}$, V is fixed. For the proton magnet with w=h=.6 cm V_p=4.3 kV and for the $\bar{p}$ magnet with w=h=1.4 cm V_p=3.5 kV. The stored energy is $W=4.4\times 10^{-14}\ \alpha^2 p_{\bar{p}}^2 wh/\ell$ and has a modest value

~6J. So we choose the magnetic field as large as possible to decrease ℓ and get the magnet as close to the lenses as possible. We choose a maximum magnetic field in the iron of 18 kG for the proton magnets permitting them to be short enough ($\ell_1=\ell_2=11.7$ cm) and relatively simple. They may be placed very close to the lens so that lens aperture is not a problem. The parameters for the pulsed current source look modest enough; the feasibility of such a supply is considered later. To choose a magnetic field of more than 15 kG for the $\bar{p}$ magnets is unreasonable because at ℓ=5 cm their inductance is already very small and it becomes difficult to eliminate the voltage loss in the parasitic inductance of the transmission line etc. The construction of the magnet is shown in Figure 8.

Pulsed Current Source

The magnet current supply can be bipolar sinesoidal current pulses from the discharge of a capacitor bank through the inductive load presented by the magnets. The magnetic field has to pass through zero to give a displacement symmetric with respect to the beam axis. For a one dimensional sweep the spill time of 1.8 μs has to be during the part of the sinesoidal pulse linear to about 10% so one can employ phase interval of $\Delta\phi\sim\pm 80°$ and so cannot use the full pulse amplitude (Fig. 9a). The pulse period must be T =2.2 μs or f=.25 mHz. For the circular sweeping the two magnets must be supplied from two sources: one switches on $\pi/2$ before the spill, the second in time with the beam (Fig. 9b). For this case the period is exactly the beam spill time $T=\Delta t=1.8$ μs and f=.55 MHz. At this frequency the pulsed current source can be built with hydrogen thyratrons and a clipper diode according to the scheme indicated in Fig. 10. Pulsed sources of this type using TI -1-1000-25 thyratrons were built at INP as early as 1972 for use with small parabolic lenses for e^+ production and collection. When used at a repetition rate of several Hz these thyratrons can commute ~10 kA at 20 kV quite reliably. Because the voltage at the magnet is not so high (V~4 kV) we propose the use of matching transformers with a turns ratio N~4 placed behind the shielding and connected to the magnets by ~2 m of low inductance (<50 nH), radiation tolerant transmission line.

References

1. T.A. Vsevolozskaya, "The Optimization and Efficiency of Antiproton Production Within a Fixed Acceptance", TM-1045 8055.00.

2. D. Cline, "The Development of Bright Antiproton Sources and High Energy Density Targeting", XI Intl Conf. High Energy Accel., CERN (July 7-11, 1980).

3. G. Bohannon, "Target Behavior Calculations", High Intensity Target Workshop, April 28-30, p. 85. We use the 1.8 μs beam spill time quoted in this reference throughout this paper for consistency. The TeV I parameters give a spill time of 1.6 μs.

4. F. Krienen and F. Mills, "Spreading the Hotspot on the Target", $\bar{p}$ Note 70, May 1980, High Intensity Target Workshop, p. 61.

References (continued)

5. EXP-101, 2/15/80 and EXP-104, 4/15/80, unpublished Fermilab Accelerator Experiment Reports.

6. T.A. Vsevolozskaya, "The Calculations of the Proton Beam Velocity Spreading for High Intensity Targeting", Unpublished report, INP Novosibirsk.

7. H. Knopfel, "Pulsed High Magnetic Fields", North Holland, London (1970).

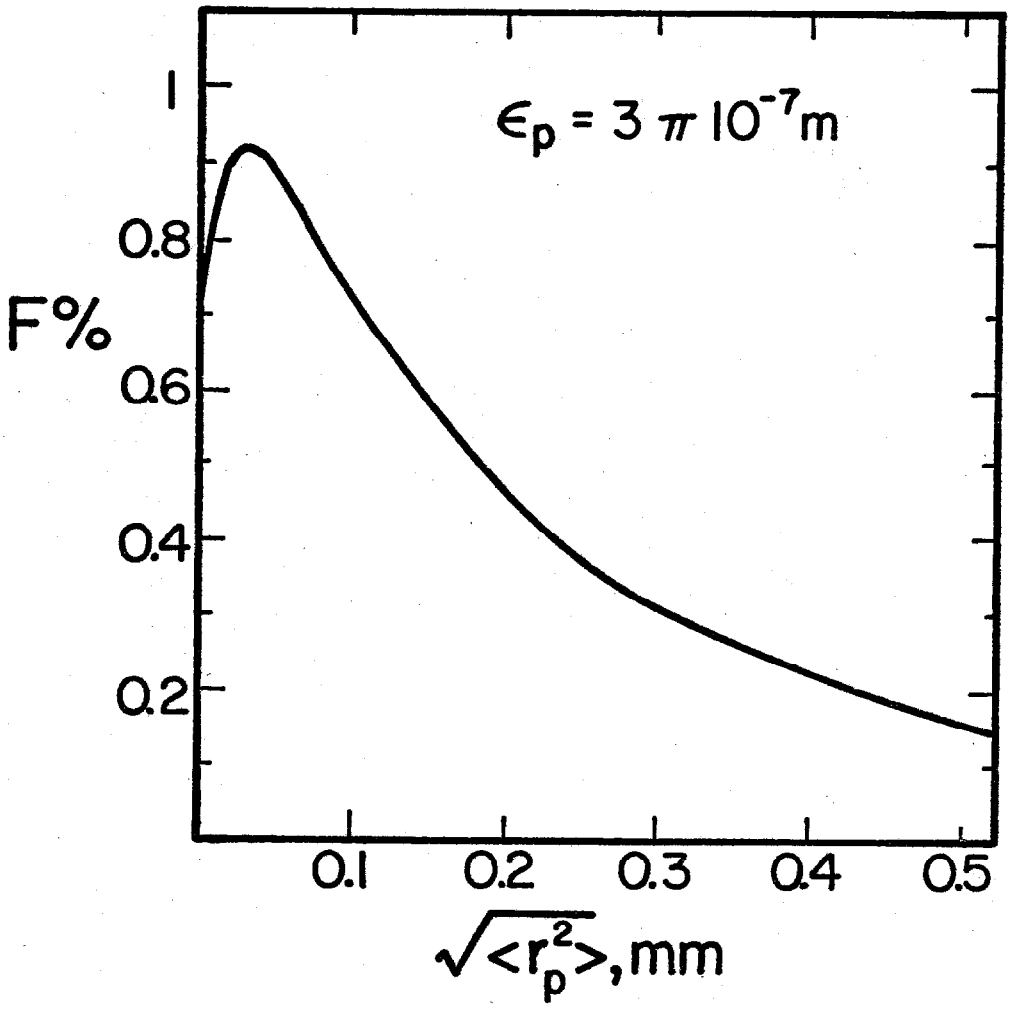

Fig. 1

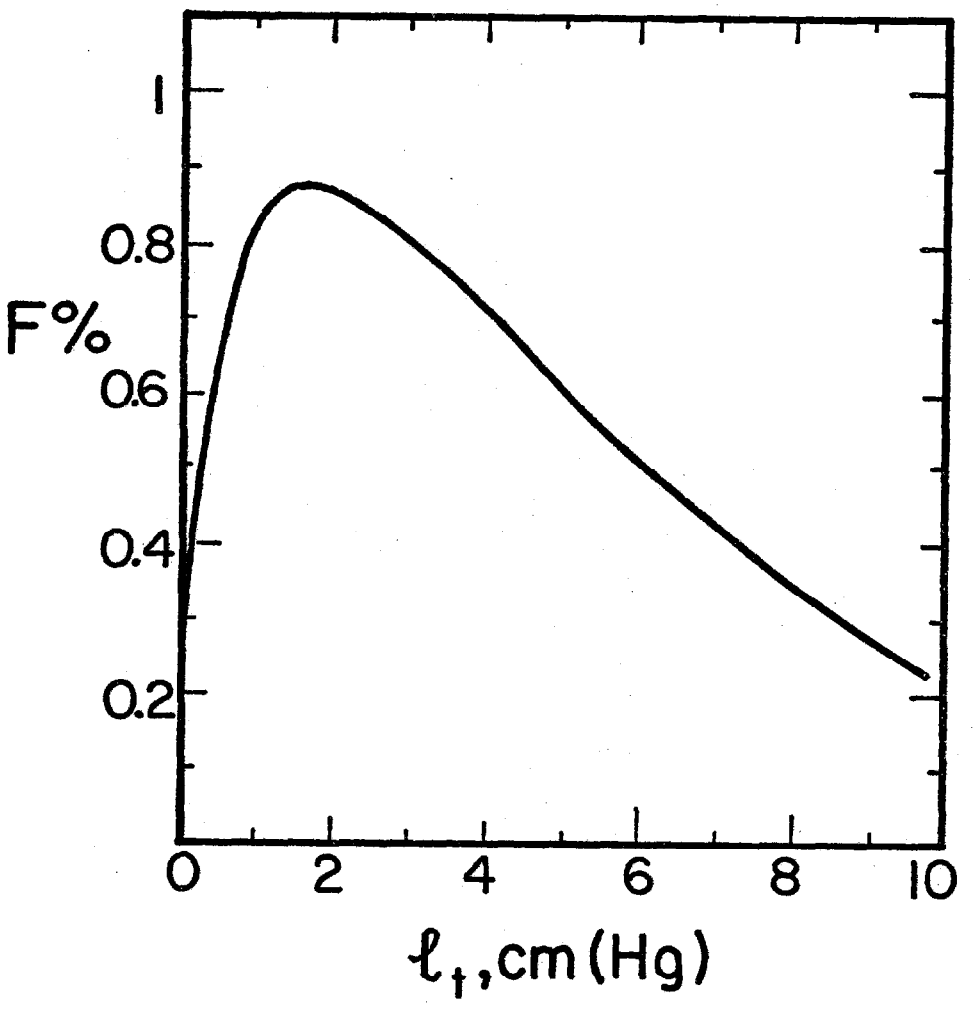

Fig. 2

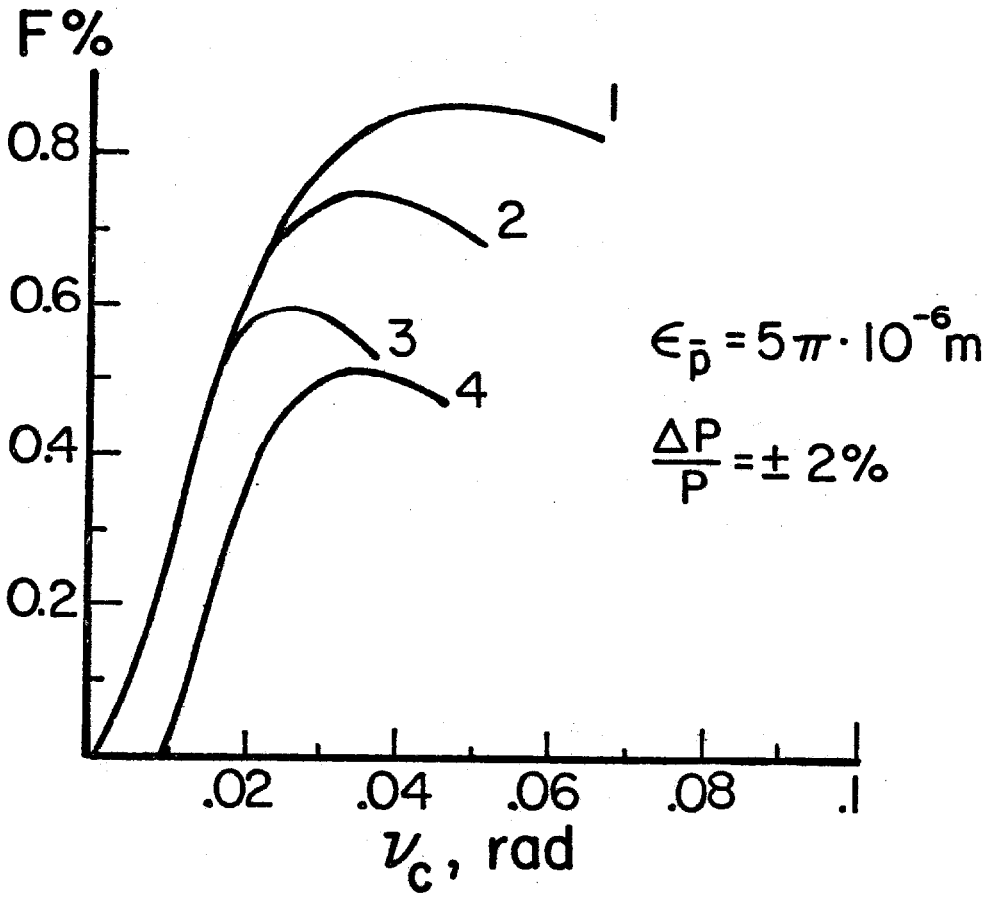

1. Ideal Lens
2. Lithium Lens with focal distance f = 10cm
   length ℓ = 7.5cm, aperture ϕ = 1 cm, G = 2800 T/m
3. Lithium Lens f = 20cm, l = 7.5cm, ϕ 2 cm
4. Linear Parabolic Lens made of Berillium

Fig.3

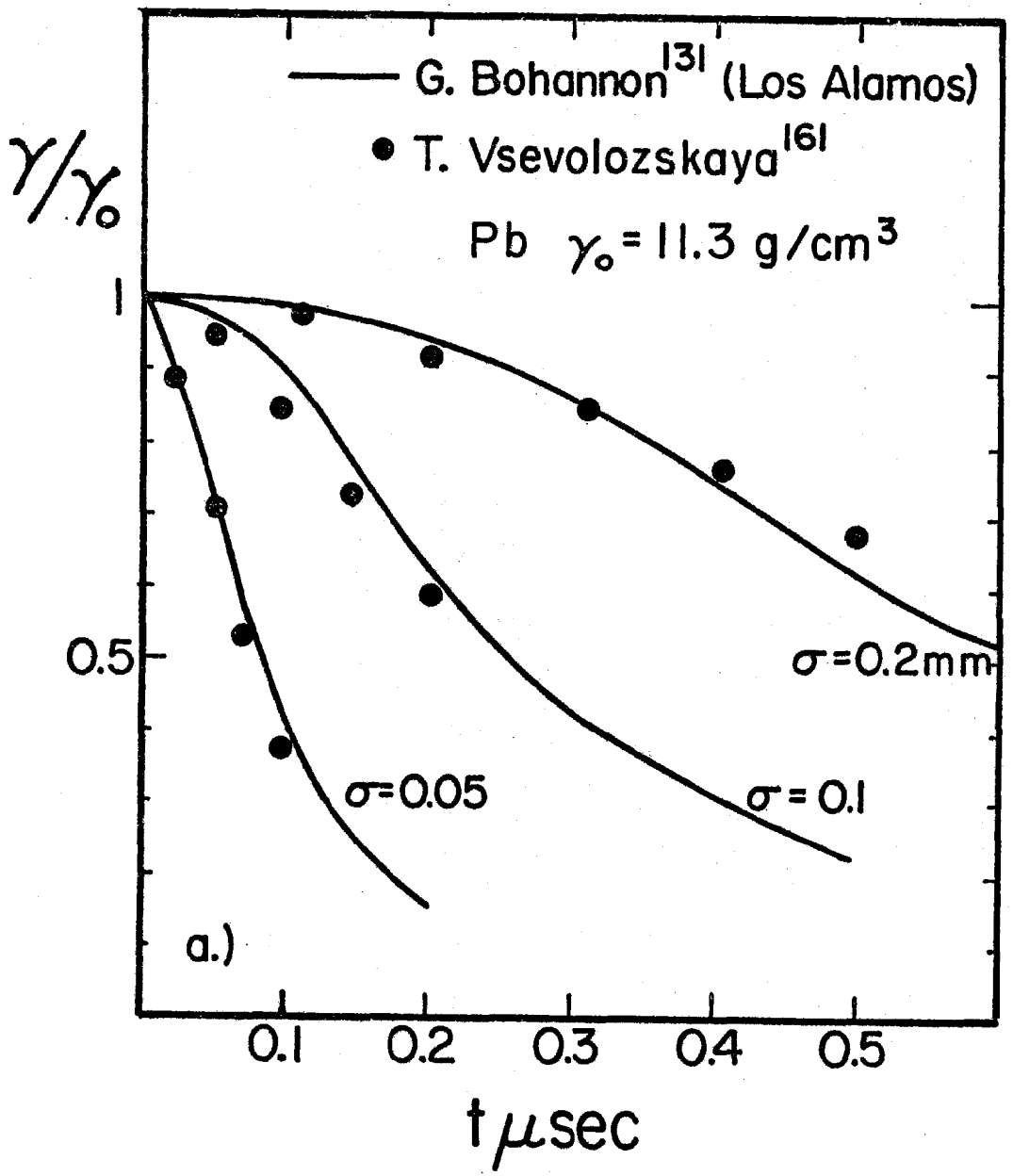
G. Bohannon[13] (Los Alamos)
T. Vsevolozskaya[16]
Pb γ_o = 11.3 g/cm^3
γ/γ_o
1
0.5
σ=0.2mm
σ=0.05
σ = 0.1
a.)
0.1
0.2
0.3
0.4
0.5
t μsec

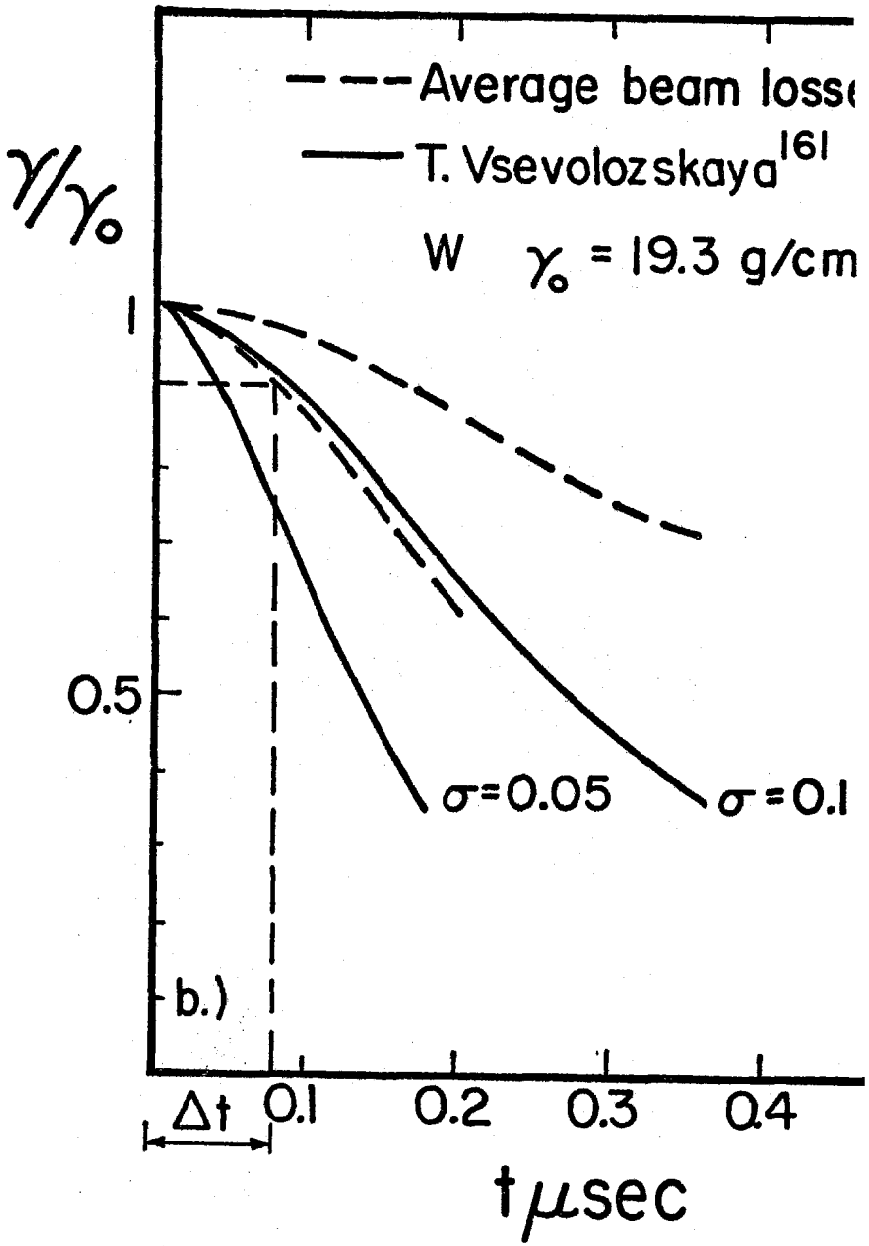
Average beam loss
T. Vsevolozskaya[16]
W γ_o = 19.3 g/cm
γ/γ_o
1
0.5
σ=0.05
σ = 0.1
b.)
Δt
0.1
0.2
0.3
0.4
t μsec

Fig. 4a-b

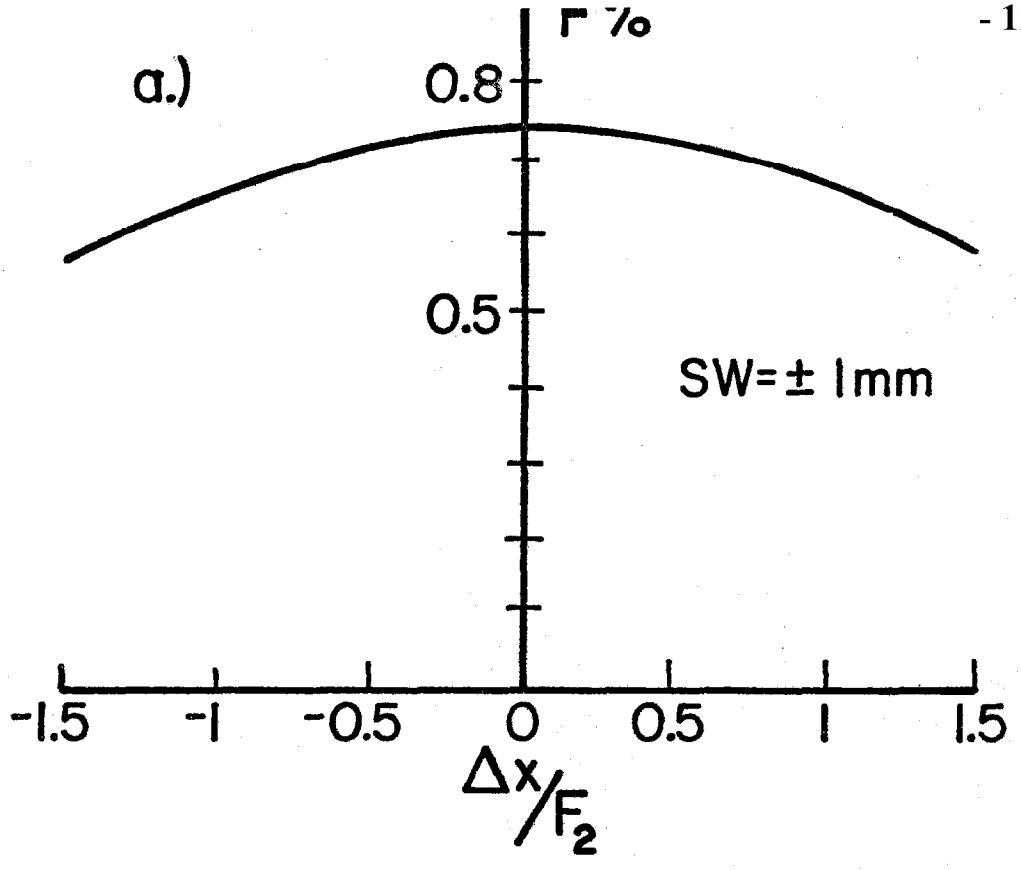
a.)
Γ %
0.8
0.5
SW=± 1mm
-1.5
-1
-0.5
0
0.5
1
1.5
Δx/F2

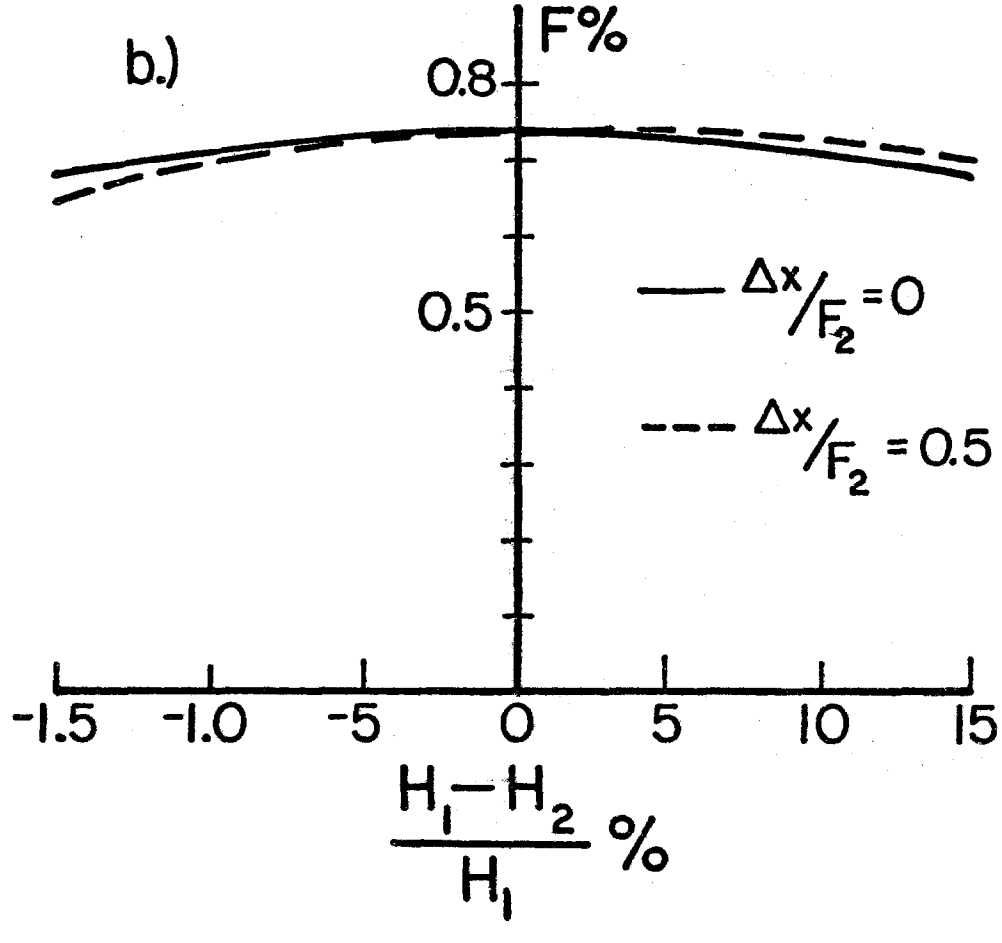
b.)
F%
0.8
0.5
Δx/F2 =0
Δx/F2 =0.5
-1.5
-1.0
-5
0
5
10
15
H1−H2 / H1 %

Fig. 5a-b

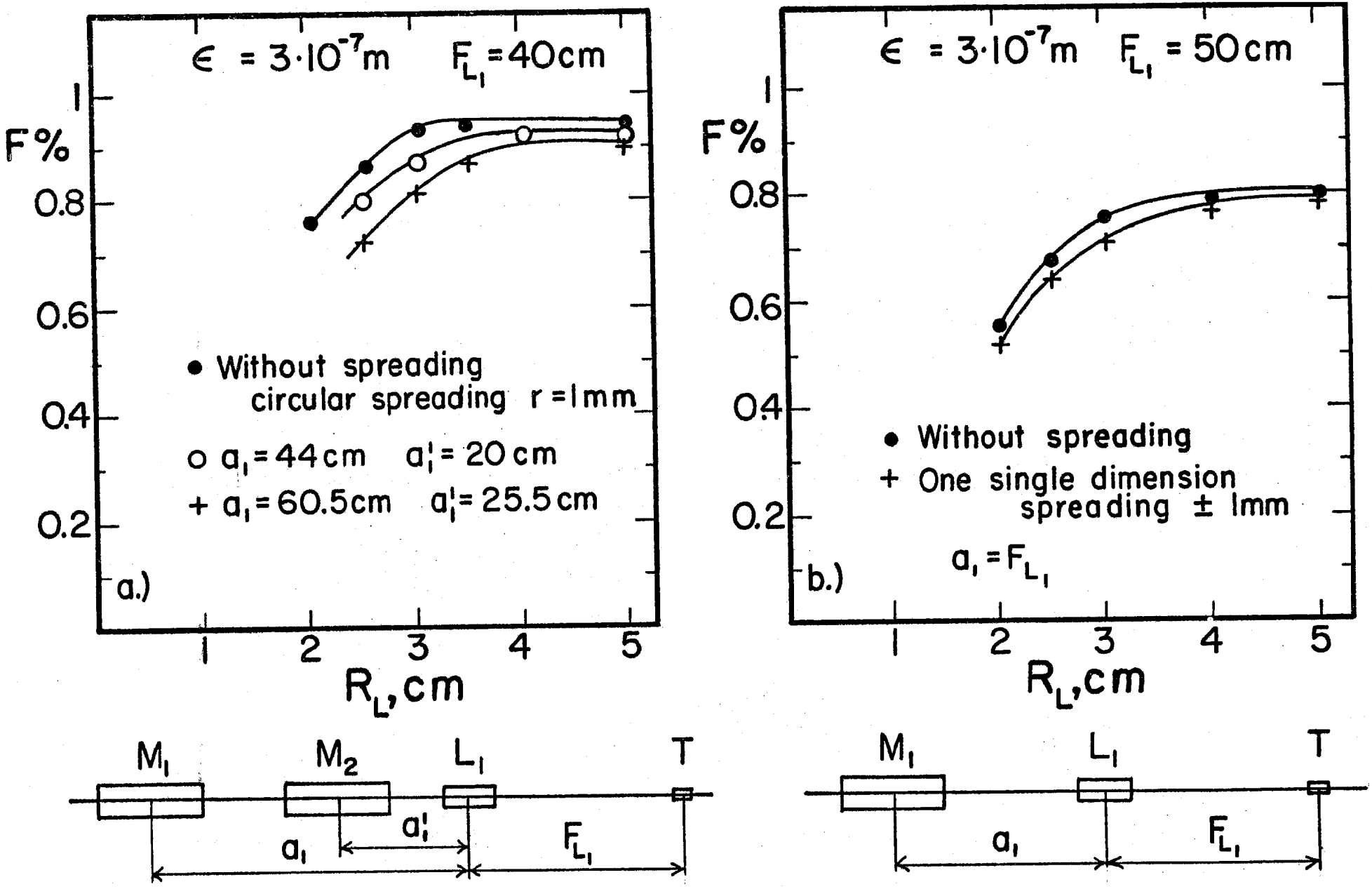
ϵ = 3·10⁻⁷m F_L1 = 40cm
F%
1
0.8
0.6
0.4
0.2
• Without spreading
circular spreading r = 1mm
o a1 = 44cm a1' = 20cm
+ a1 = 60.5cm a1' = 25.5cm
a.)
1 2 3 4 5
R_L, cm
ϵ = 3·10⁻⁷m F_L1 = 50cm
F%
1
0.8
0.6
0.4
0.2
• Without spreading
+ One single dimension
spreading ± 1mm
a1 = F_L1
b.)
1 2 3 4 5
R_L, cm
M1 M2 L1 T
a1
a1'
F_L1
M1 L1 T
a1
F_L1

Fig. 6a–b

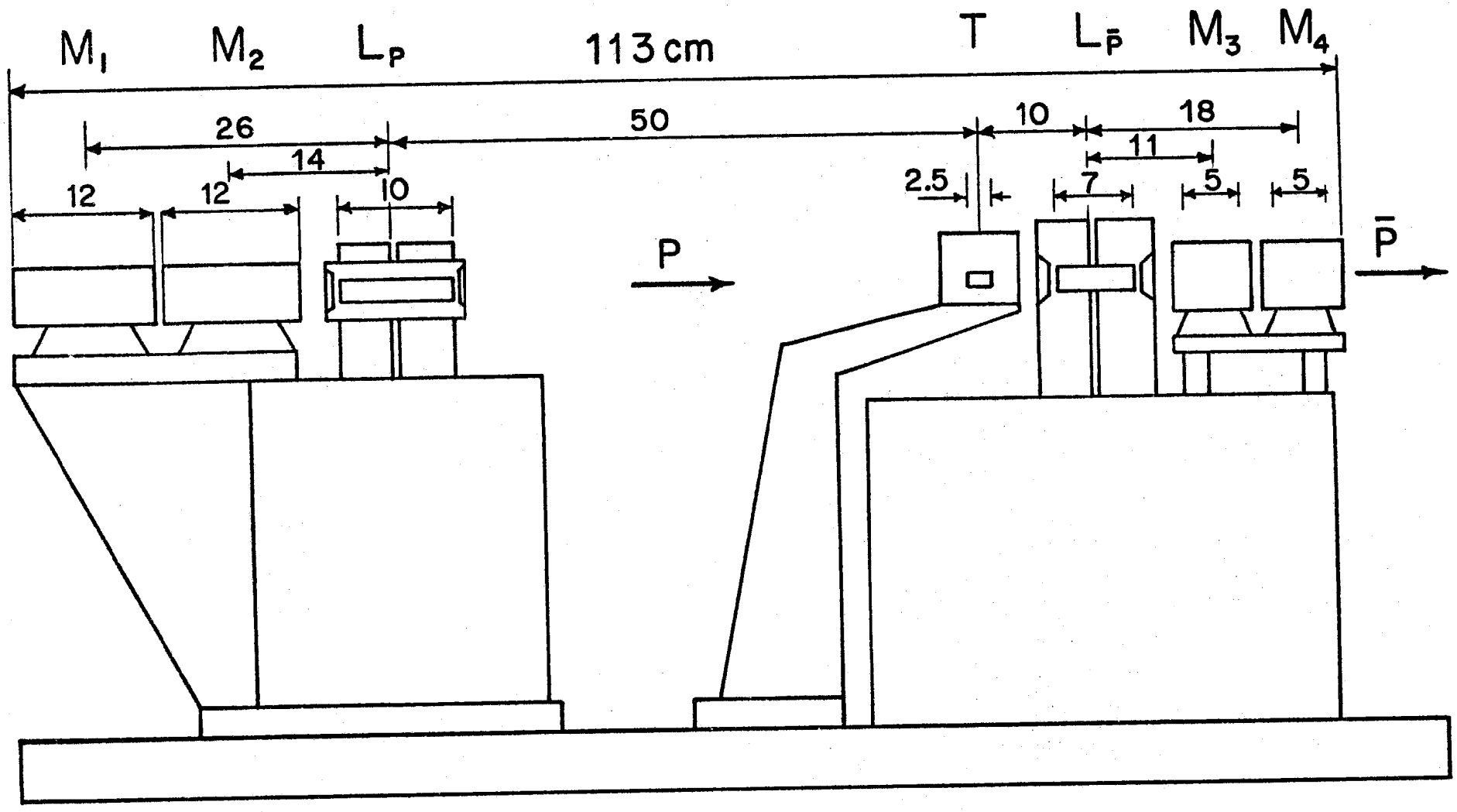

Fig. 7

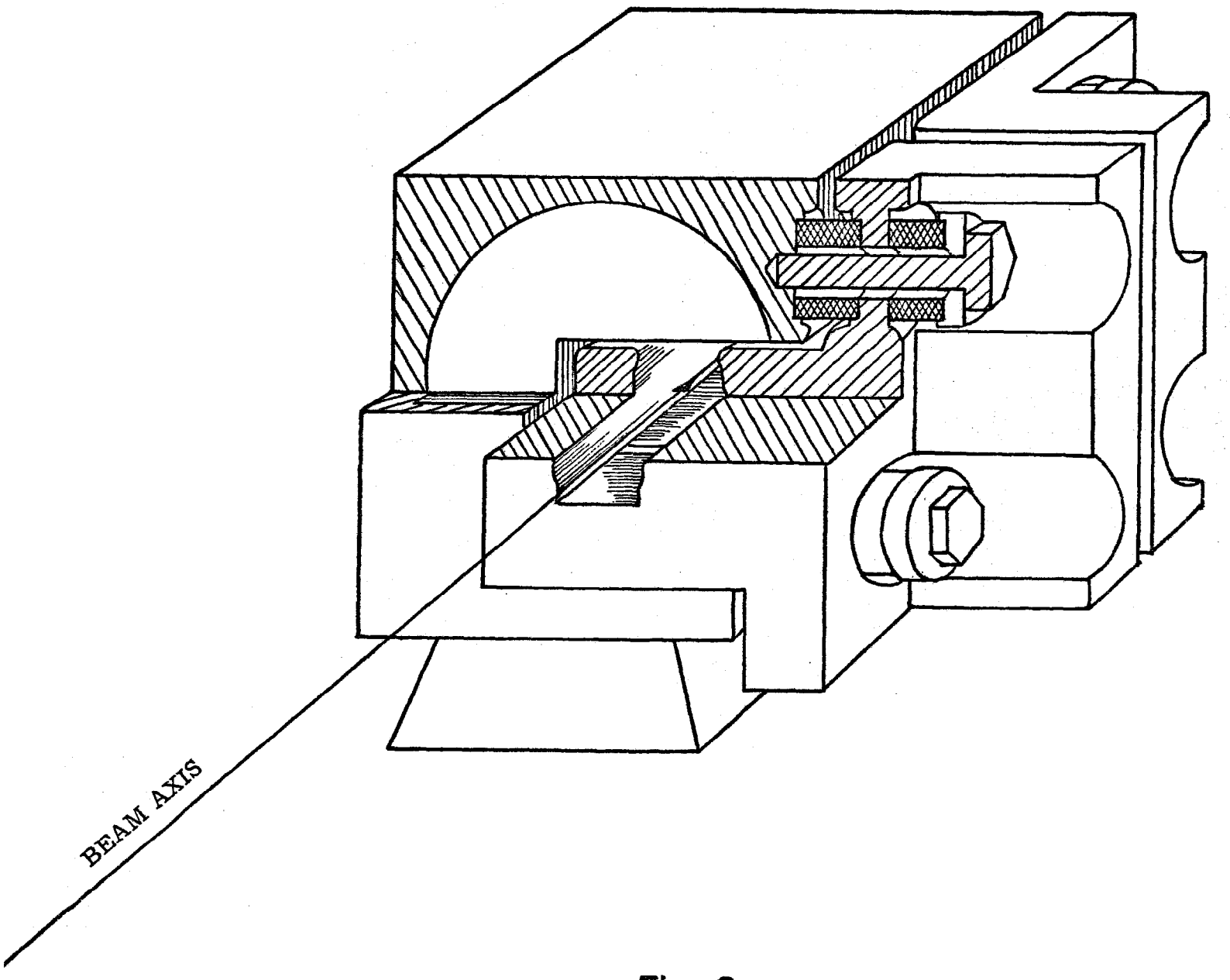

Fig. 8a

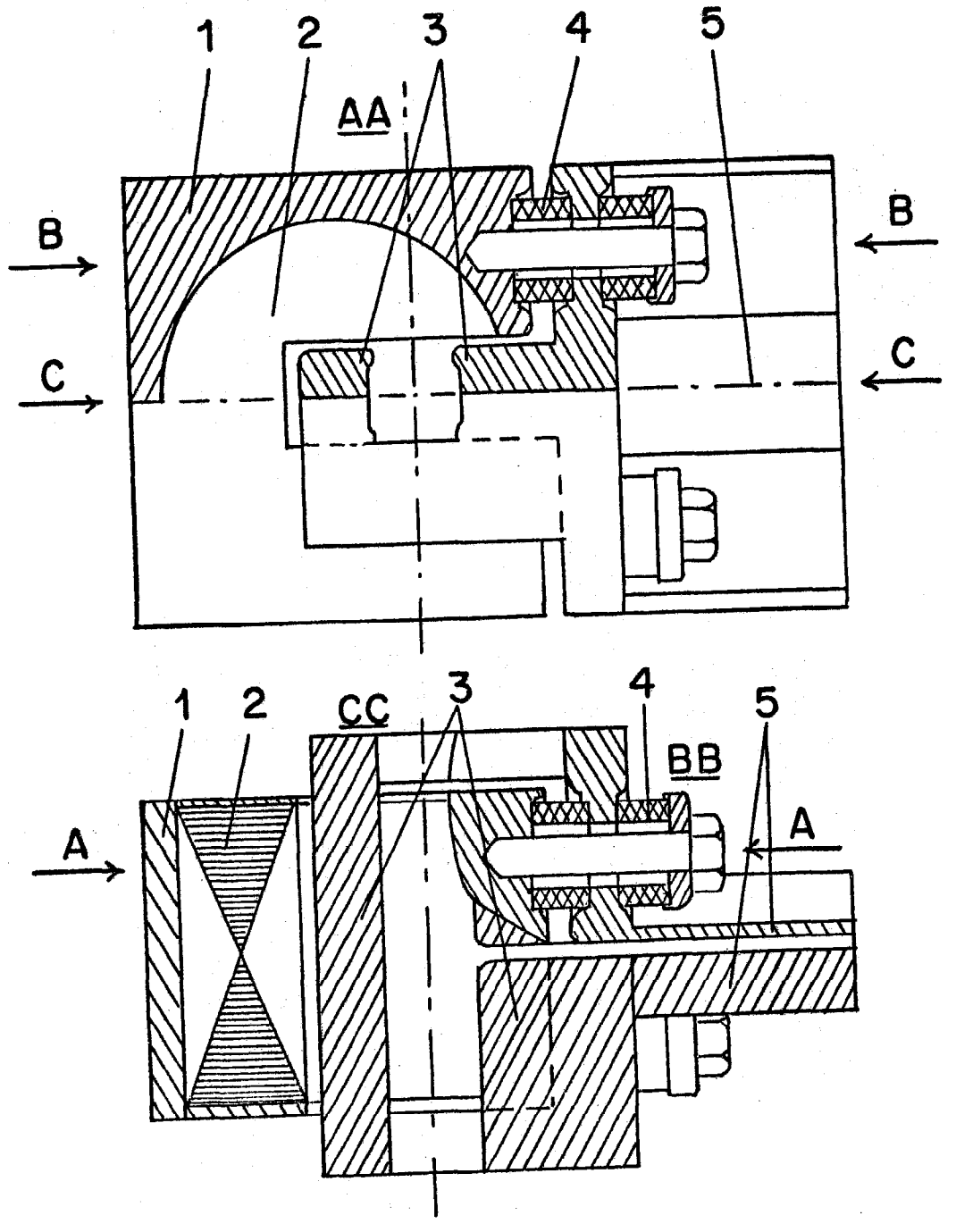

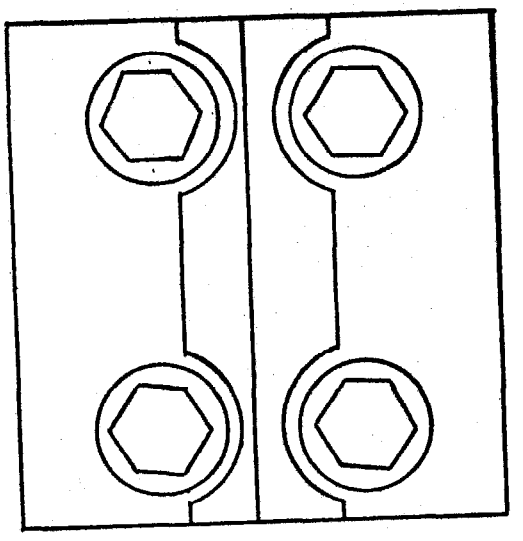

1. Iron Case
2. Laminated Iron Core
3. Copper Conductor
4. Ceramic Insulator
5. Stripline Current Input

Fig. 8b

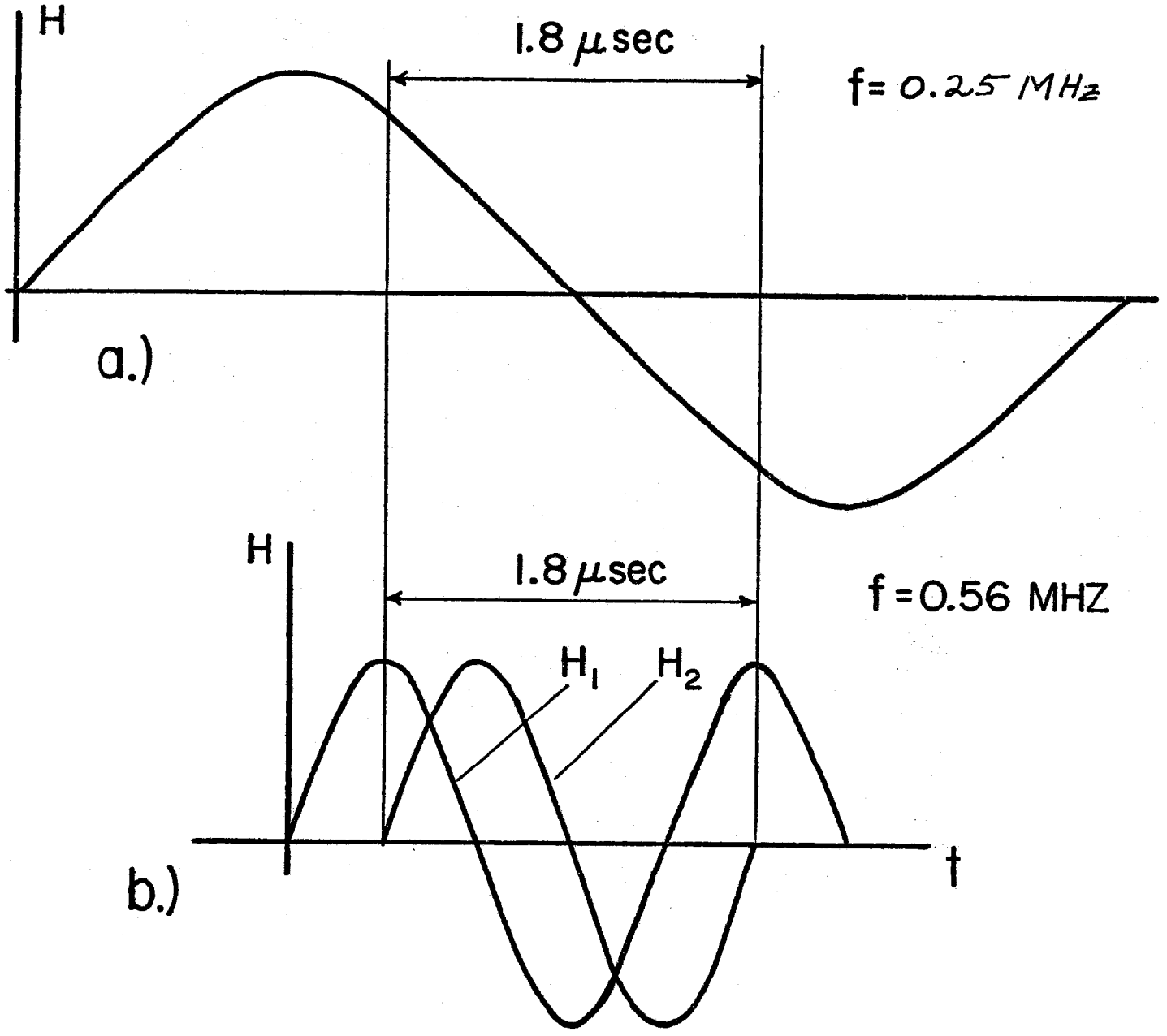

Fig. 9 a–b

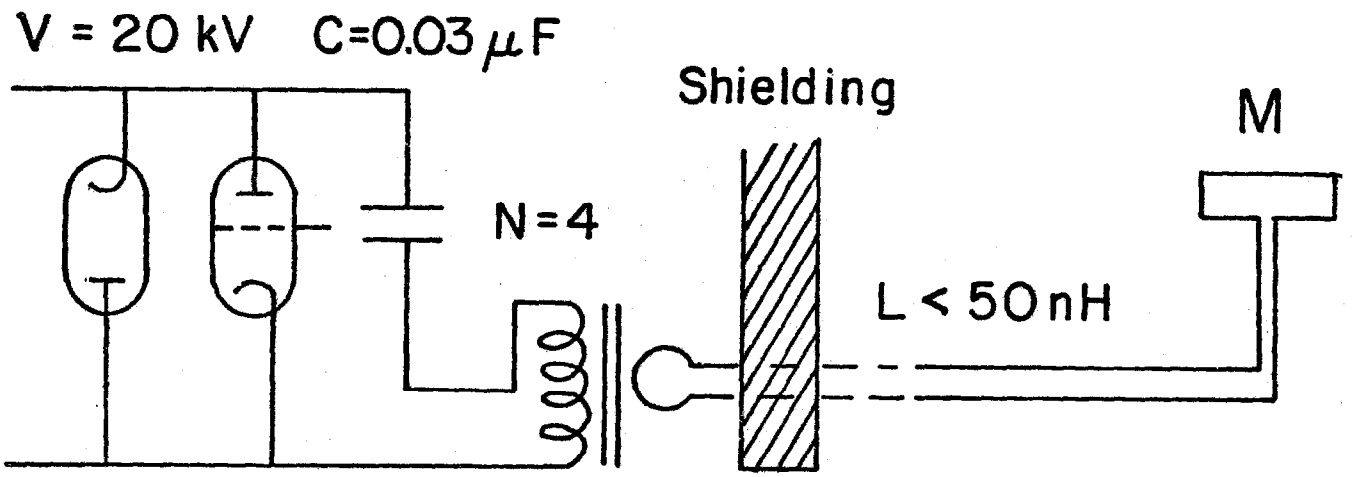

Fig. 10